Using MAGIC to Validate and Optimize Interferometers

Erick Leon[1]

I. INTRODUCTION

In 1915 Albert Einstein put forward his theory of general relativity; a theory meshing together space and time into an entity called space-time. Einstein predicted the existence of gravitational waves: ripples in space-time that stretch and squeeze space as these waves pass through it. Gravitational waves can be caused by merging binaries, such as two black holes colliding. In 2015 this binary collision is exactly what the gravitational wave community detected: confirming Einsteins theory of general relativity. Einstein, however, did not believe that scientists would be able to detect these gravitational waves because the fractional change in distance that they cause would be incredibly small. Modern marvels in physics are the adapted Michaelson-Morley interferometers used to detect these gravitational waves.

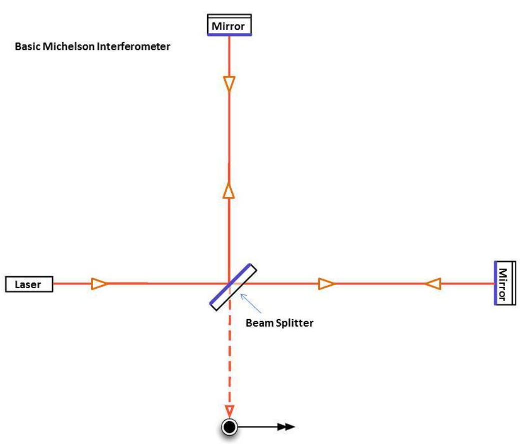

Fig. 1: Diagram of the basic Michaelson Interferometer

They include two arms perpendicular to each other which stretch and squeeze as gravitational waves pass through them. Currently, LIGO (Laser Interferometer Gravitational-Wave Observatory) has two interferometers, both equipped with 4km arms, and are stationed in the United States. VIRGO is equipped with 3km arms and is stationed in Italy. With these grand interferometers, scientists are able to detect fractional changes in lengths of about 10^{-21}, which is about a thousandth the size of a proton

II. MOTIVATION

Interferometers are searching for disturbances in the interference pattern caused by the interfering light rays coming from the two arms solely caused by gravitational waves. However, there are other disturbances that can cause interference patterns and may disturb the interferometer in such a way as to make the gravitational waves undetectable. These are known as noise sources and can be caused by a variety of physical sources. Knowing how these sources affect the interferometers in the frequency range is important in order to distinguish gravitational waves from the total signal which includes noise. The Modular and Adaptable Gravitational-wave Interferometer noise Calculator (MAGIC) which was developed at the University of Birmingham is a python implementation of FINESSE (Frequency domain INterfErometer Simulation SoftwarE). MAGIC is used to calculate noise curves based on the design of aLIGO, Voyager, or the Einstein Telescope where the user can change parameters of a chosen interferometer, such as mirror mass, laser power, etc. and get a resultant noise curve. With the resultant noise curve we can calculate how far the detector with these new parameters can accurately detect gravitational waves from a binary system of varying parameters. By using MAGIC we can then look for which parameters best suit the interferometer for detecting a selected set of binaries described by the individual masses. The aim of this project is to use MAGIC in order to validate the Voyager and Einstein Telescope noise curve and predict what should be the optimal parameters of the Voyager update to aLIGO.

III. QUANTUM NOISE

Part of our research was understanding how changing the parameters of a detector in MAGIC changed the total noise of the detector. The most dominant noise in the high frequency range is quantum noise, also known as shot noise in the high frequency regime. It is also very limiting in the low frequency where it is referred to as radiation pressure noise. To understand this noise we must delve into quantum mechanics. The following derivation of quantum noise for a simple mirror system was worked out originally by our advisor Dr. Hiaxing Miao [1].

A. THE ELECTRIC FIELD

We may describe the electric field operator as:

$$\hat{E} = u(x,y,z)\int_0^\infty \frac{d\omega}{2\pi}\sqrt{\frac{2\pi\hbar\omega}{\mathcal{A}c}}[\hat{a}_\omega e^{ikz-i\omega t} + \hat{a}^\dagger_\omega e^{-ikz+i\omega t}] \tag{1}$$

Where $\hat{a}^\dagger_\omega$ and $\hat{a}_\omega$ represent the creation and annihilation operators, $\mathcal{A}$ being the cross-sectional area of the laser and $u(x,y,z)$ is a function dependent on the area such that the integral of $u(x,y,z)^2$ divided by $\mathcal{A}$ is equal to one. We can then take combinations of $\hat{a}^\dagger_\omega$ and $\hat{a}_\omega$ to represent two photons being created and destroyed in the lower and upper sidebands,

$$\hat{a}_+ = \hat{a}_{\omega_0+\Omega} \tag{2}$$

$$\hat{a}_- = \hat{a}_{\omega_0-\Omega} \tag{3}$$

We can then take combinations of these operators to create more meaningful ones, namely:

$$\hat{a}_1 = (\hat{a}_+ + \hat{a}^\dagger_-)/(\sqrt{2}) \tag{4}$$

$$\hat{a}_2 = (\hat{a}_+ - \hat{a}^\dagger_-)/(i\sqrt{2}) \tag{5}$$

Now we may rewrite the electric field operator in terms of these new combinations. The electric field is then represented as:

$$\hat{E} = u(x,y,z)\sqrt{\frac{4\pi\hbar\omega}{\mathcal{A}c}}[\hat{a}_1(z,t)e^{-i\Omega t+ikz} + \hat{a}_2(z,t)e^{i\Omega t-ikz}] \tag{6}$$

Here $\hat{a}_1$ and $\hat{a}_2$ represent the amplitude and phase operators respectively.

B. CAVITIES AND MIRROR SURFACES

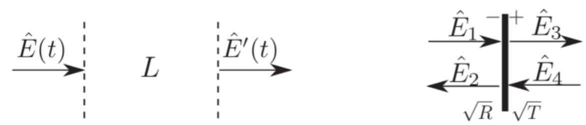

Fig. 2: Electric field: free propagation and reflectance and transmittance

Now that we have defined the electric field in such a way, we may look at a system such as a cavity where light is propagating in free space or where light is being reflected and transmitted, and describe the final electric field in terms of the input one(s) such as the figure above. It turns out that the behavior of these systems looks a lot like the classical approach. Namely

$$\hat{E}'(t) = \hat{E}(t-\tau), \tag{7}$$

where $\tau = L/c$, and

$$\hat{E}_2 = \sqrt{T}\hat{E}_4 - \sqrt{R}\hat{E}_1(t) \tag{8}$$

$$\hat{E}_3 = \sqrt{R}\hat{E}_4 + \sqrt{T}\hat{E}_1(t). \tag{9}$$

Here, T and R are the transmissivity and reflectivity.

C. APPLICATION TO A MOVING MIRROR AND QUANTUM NOISE

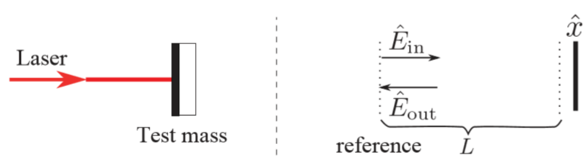

Fig. 3: Diagram of the propagation of the electric field through free space and its reflection off of a moving mirror

We are now ready to apply our knowledge of electric fields to a setup involving free space propagation as well as some small propagation caused by a small displacement of the mirror by an incoming gravitational wave (3). The incoming beam can be written as

$$\hat{E}(t)_{in} = [\sqrt{\frac{2I_0}{\hbar\omega_0}} + \hat{a}_1(t)]\cos(\omega_0 t) + \hat{a}_2(t)\sin(\omega_0 t), \quad (10)$$

where $\sqrt{\frac{2I_0}{\hbar\omega_0}}$ corresponds to the macroscopic laser power, whcih gives the electric field its macroscopic amplitude. The reflected beam which travels a distance $2L/c$ (twice the cavity length) and $2\hat{x}/c$ (twice the mirror displacement) can be written as

$$\hat{E}(t)_{out} = \hat{E}_{in}(t - 2\tau - 2\hat{x}/c), \quad (11)$$

where $\tau = L/c$. We can assume that the length of the cavity is an integer multiple of the product $\frac{\omega_0 L}{c}$, which gets rid of the term involving L inside the sin and cos. Also, due to the fact that the displacement of the mirror is small, we may approximate the equation above and arrive at

$$\hat{E}(t)_{out} = [\sqrt{\frac{2I_0}{\hbar\omega_0}} + \hat{b}_1(t)]\cos(\omega_0 t) + \hat{b}_2(t)\sin(\omega_0 t), \quad (12)$$

where

$$\hat{b}_1(t) = \hat{a}_1(t - 2\tau), \quad (13)$$

$$\hat{b}_2(t) = \hat{a}_2(t - 2\tau) - 2\sqrt{\frac{2I_0}{\hbar\omega_0}}\frac{\omega_0}{c}\hat{x}(t - \tau). \quad (14)$$

Here, $\hat{b}_1$ and $\hat{b}_2$ correspond to the output amplitude and phase operators in terms of $\hat{a}_1$ and $\hat{a}_2$: the input amplitude and phase operators. We must now solve for the displacement of the mirror $\hat{x}$. We may do so by solving the equation of motion for the mirror which involves the radiation pressure force as well as the acceleration of the mirror caused by the gravitational wave strain,

$$m\ddot{\hat{x}}(t) = \hat{F}_{rp}(t) + \frac{1}{2}mL\ddot{h}(t), \quad (15)$$

where

$$\hat{F}_{rp}(t) = \frac{2I_0}{c}[1 + \sqrt{\frac{2\hbar\omega_0}{I_0}}\hat{a}_1(t - \tau)]. \quad (16)$$

We can solve these equations by doing a Fourier transform into the frequency domain. Here the output amplitude and phase operators are

$$\hat{b_1}(\omega) = e^{2i\Omega\tau}\hat{a_1}(\Omega), \quad (17)$$

$$\hat{b_2}(\omega) = e^{2i\Omega\tau}(\hat{a_2}(\Omega) - (\tfrac{8I_0\omega_0}{mc^2\Omega^2})\hat{a_1}(\Omega) + e^{i\Omega\tau}\sqrt{\tfrac{2I_0\omega_0}{\hbar}}h(\Omega). \quad (18)$$

We can see from this equation that the gravitational wave signal is contained in the output phase operator. We can now represent this output phase operator in terms of its expectation value and its uncertainty, in other words, in its signal and noise:

$$\hat{b}_2(\Omega) = <\hat{b}_2(\Omega)> + \Delta\hat{b}_2(\Omega). \quad (19)$$

The expectation value of the output phase operator can be defined as $<\hat{b}_2(\Omega)> = \mathcal{T}h$ where

$$\mathcal{T} = e^{i\Omega t}\sqrt{2\frac{I_0\omega_0 L^2}{\hbar c^2}}. \quad (20)$$

This is the transfer function which transforms the gravitational wave strain into the output phase operator. With this transfer function it can be shown that the noise can be written as

$$\Delta\hat{b}_2(\Omega) = e^{2i\Omega\tau}\hat{a}_2(\Omega) - \frac{8I_0\omega_0}{mc^2\Omega^2}e^{2i\Omega\tau}\hat{a}_1(\Omega). \quad (21)$$

This first term in the equation corresponds to the shot noise, which is caused by fluctuations of the input phase operator. In terms of the photons, the shot noise arises due to the fact that the photons are coming in at random times, and there is an uncertainty in the number of photons arriving. The second term corresponds to the input amplitude operator and its uncertainty. Since the photons arrive randomly, the pressure will vary randomly as well, this is the radiation pressure noise. The shot noise and radiation pressure noise power spectrum can be summed up as

$$S^h(\Omega) = [\frac{1}{\xi I_0} + \xi I_0]\frac{h^2_{SQL}}{2}, \tag{22}$$

where

$$\xi = \frac{8\omega_0}{mc^2\Omega^2} \quad , \quad h_{SQL} = \sqrt{\frac{8\hbar}{m\Omega^2 L^2}}. \tag{23}$$

In equation 22, the first term is the shot noise and the second term is the radiation pressure noise. It is clear that the shot noise depends inversely with the laser power, and the radiation pressure is proportional to the laser power. This simple example of quantum noise and the relationship with power can be generalized to more complicated systems, including the Michaelson-Morly interferometer of aLIGO, Voyager and even the Einstein Telescope models. This analysis helps us build an intuition on how quantum noise depends on laser power, which is a key component in any interferometer.

IV. MAGIC

A. *PURPOSE OF MAGIC*

MAGIC is a python implementation of the program FINESSE created by Isobel Romero-Shaw and Roshni Vincent [3], [4]. This program is used to model complicated interferometers as to analyze many import aspects of the system such as laser power at a point or the displacement of a mirror due to radiation pressure. MAGIC is primarily used to plot noise curves for any given interferometer. In MAGIC, there are preloaded interferometer schematics corresponding to aLIGO, Voyager, Einstein Telescope, and Cosmic Explorer. These schematics are python implementations of the same schematics on FINESSE. With this python implementation however, there is a much more user friendly way to change the parameters of any chosen interferometer including laser power, mirror transmittances, cavity lengths, etc.

The user can change the parameters as they see fit and see how the noise changes. This includes, the individual noises such as quantum noise, thermal noise, Newtonian noise, etc. Our project involved working on certain applications of MAGIC, and attempting to justify it as an accurate noise calculator.

B. *APPLICATIONS: aLIGO VALIDATION*

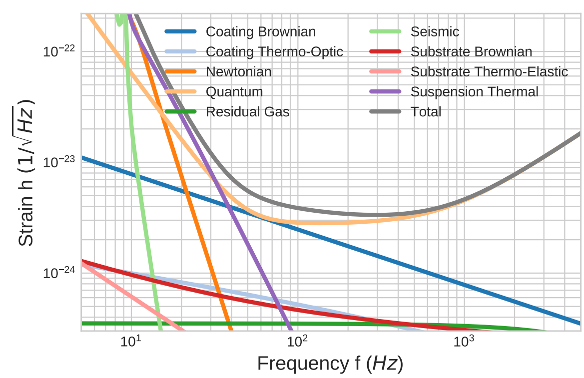

Fig. 4: aLIGO Noise Curve.

Advanced LIGO is an established interferometer based in the United States which has successfully detected a variety of gravitational waves, included those from binary black holes and binary neutron star mergers. We plotted the aLIGO curve produced by MAGIC with the noise curve provided through LIGO and were pleased to find that there was a great similarity between the curves.

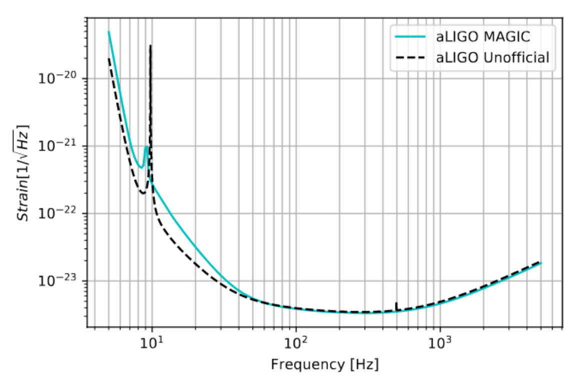

Fig. 5: aLIGO Validation.

The only discrepancy seems to lie in the low frequency range where we believe that there is a resonance in the mirror suspensions that are accounted for in the LIGO data, but not in the MAGIC implementation.

C. VOYAGER VALIDATION

The Voyager update to advanced LIGO is said to be the final upgrade before implementing the next generation of gravitational wave detectors. Voyager is said to involve cryogenic cooling to its mirrors, as well as a larger mirror mass, and a silica coating. Indeed in MAGIC these parameters are specified in the code explicitly, along with other parameters shared with aLIGO such as arm length. We plotted the noise curve of Voyager using MAGIC and compared this curve to data acquired from LIGO (figure below).

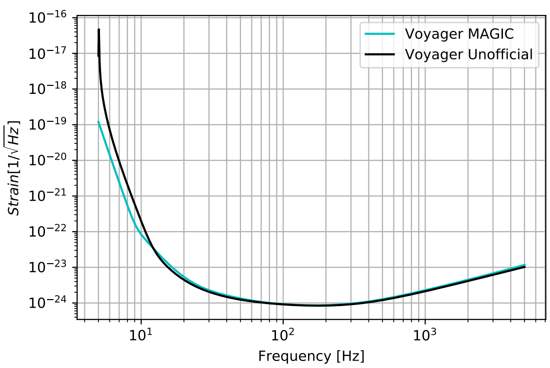

Fig. 6: Voyager validation.

D. EINSTEIN TELESCOPE VALIDATION

The Einstein Telescope is said to be part of the next generation of advanced interferometers. It consists of three 10 km arms at 60 degrees apart, totaling three interferometers in this configuration. This allows for the two polarizations of the gravitational wave that are 45 degrees to each other to be detected.

Another reason is that it allows scientists to use two different laser powers: one at low power to investigate the low frequency regime where radiation pressure noise dominates, and one at high power to investigate the high frequency regime where shot noise dominates. This combination results to an overall lower noise curve compared to aLIGO and Voyager. However, in our investigation of the Einstein Telescope noise curve created by MAGIC, we were not able to resolve the issue of the noise curve being significantly higher than the noise curve acquired through LIGO.

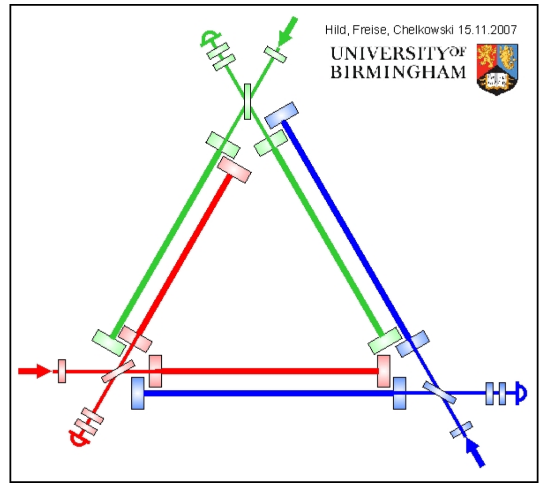

Fig. 7: Einstein telescope configuration.

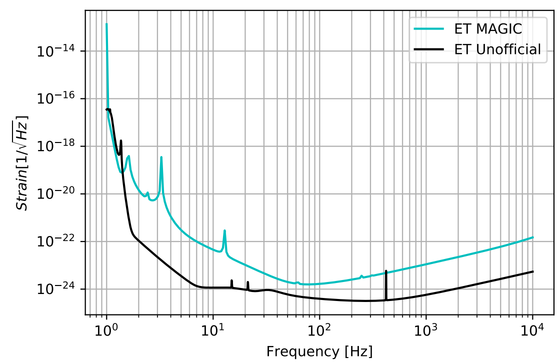

Fig. 8: Einstein Telescope validation

V. OPTIMIZATION THROUGH DIFFERENTIAL EVOLUTION

One of the main purposes of MAGIC is being able to change the parameters of an interferometric system and produce the corresponding noise curve. With any configuration such as Voyager, we are able to change the parameters to look for a better noise curve, where the definition of a better noise curve lies in the signal to noise ratio of the gravitational wave strain and the noise curve. This signal to noise ration also corresponds to how far the interferometer can detect the corresponding binary. This signal to noise ratio depends on not only the noise curve, but also the gravitational wave strain, which depends on what kind of binary system is producing the strain. In our investigations of optimizing Voyager and Einstein Telescope, we look at strains produced by phenomenological models [2] of a 25 solar mass binary (representing a black hole binary) and a 1.4 solar mass binary (representing a neutron star binary). It would be tedious to manually change the parameters of the noise curve and look for the best distance the interferometer can detect. Instead, there is a script implemented in MAGIC which takes advantage of the function differential evolution, which goes through iterations of parameter space (choosing mirror mass, suspension length, laser power,etc.), getting distances, then chooses the next iteration on whether the previous iteration produced a better or worse distance. The function looks through parameter space, looking to maximize the distance than the previous one. This is an improved method of searching for optimal parameters, because the code chooses the next parameters based on information provided by the previous set of parameters. We use this method to optimize Voyager and Einstein Telescope.

A. VOYAGER OPTIMIZATION

Below are the graphs of the optimizations of Voyager for a 25 solar mass binary system as well as for a 1.4 solar mass binary system.

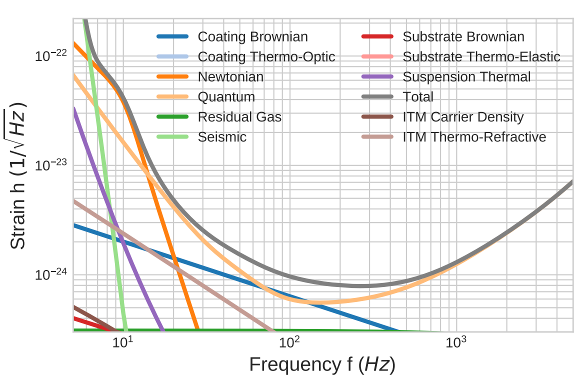

Fig. 9: Optimized noise curve of Voyager for a dual 25 solar mass binary system

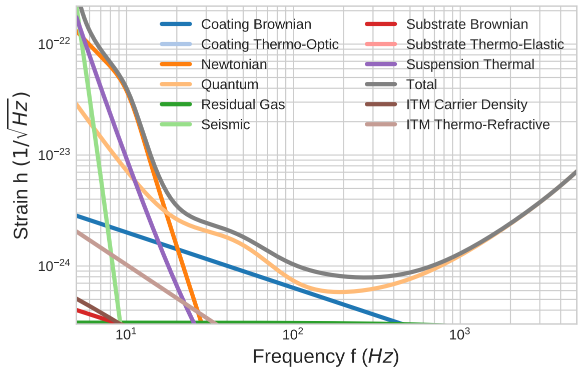

Fig. 10: Optimized noise curve of Voyager for a dual 1.4 solar mass binary system

Each optimization produces a lower noise curve than the original MAGIC Voyager noise curve. The parameters for each Voyager optimization are listed below

	25-25	1.4-1.4
Power (W)	298	300
Sus_len_4 (m)	1.16	2.55
Mass_4 (kg)	260	263
srm_transmittance	0.0238	0.0234

Fig. 11: List of parameters for Optimized Voyager noise curves for 25 SM and 1.4 SM binary systems. Where suspension length and mirror mass listed correspond to the final mirror in the python arrays of these variables.

B. EINSTEIN TELESCOPE OPTIMIZATION

The graphs of the optimizations for the Einstein Telescope for a 25 solar mass binary system and for a 1.4 solar mass binary system

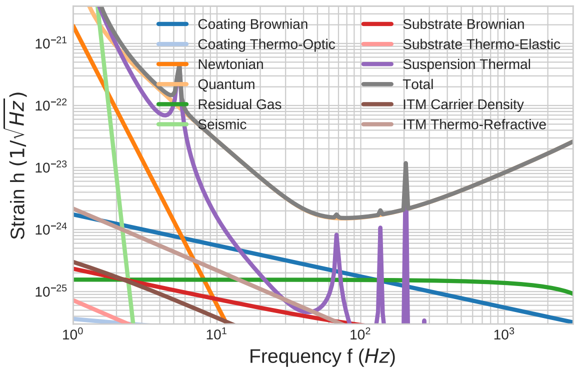

Fig. 12: Optimized noise curve of ET for a dual 25 solar mass binary system

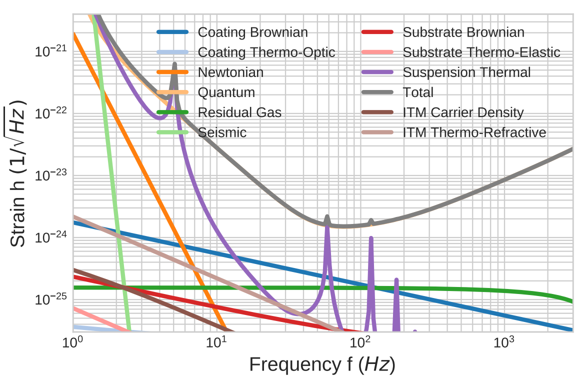

Fig. 13: Optimized noise curve of ET for a dual 1.4 solar mass binary system

The optimized curves for Einstein Telescope are lower than the noise curve of the Einstein Telescope produced by its original set of parameters. A table showing these parameters compared to the optimized parameters are shown below.

	25-25	1.4-1.4
Power (W)	300	300
Sus_len_4 (m)	1.59	1.85
Mass_4 (kg)	300	300
srm_trans mittance	0.038	0.040

Fig. 14: List of parameters for Optimized ET noise curves for 25 sM and 1.4 SM binary systems. Where suspension length and mirror mass listed correspond to the final mirror in the python arrays of these variables.

VI. CONCLUSION

We have derived for ourselves the quantum noise for a simple system, whose results are found in [1]. This let us build an intuition on how laser power affects the quantum noise, which is one of the most important limiting factor at low frequencies, and the most dominant in high frequencies. We then used MAGIC to validate aLIGO, Voyager and partially the Einstein Telescope. Although, some more work needs to be done to resolve the discrepancy between the MAGIC implementation and the LIGO implementation of the Einstein Telescope noise curve. A final implementation of MAGIC was an attempt to optimize Voyager and Einstein Telescope specifically for dual binaries of 25 and 1.4 solar masses. This code is an important and powerful tool to deduce the efficiency of interferometers, and will hopefully in the future influence a discussion on a do-it-all interferometer noise calculator.

REFERENCES

[1] Haixing, Mao. Exploring Macroscopic Quantum Mechanics in Optomechanical Devices (2010)

[2] Ajith P., et al., 2009, Phys.Rev.D., doi:10.1103/PhysRevD.77.10401710.1103/PhysRevD.79.129901

[3] Isobel Romero-Shaw, (2018) ”A Modular and Adaptable Gravitational Wave Interferometer Noise Calculator”

[4] Roshni Vincent,(2018) ”The use of a new Modular and Adaptable Gravitational wave Interferometer noise Calculator in Designing High Frequency Detectors”